IET Nanobiotechnology

Research Article

IET Journals
The Institution of Engineering and Technology

Luteinizing hormone-releasing hormone targeted poly(methyl vinyl ether maleic acid) nanoparticles for doxorubicin delivery to MCF-7 breast cancer cells

ISSN 1751-8741
Received on 13th July 2015
Revised on 12th October 2015
Accepted on 26th October 2015
doi: 10.1049/iet-nbt.2015.0056
www.ietdl.org

Jaleh Varshosaz[1] ✉, *Ali Jahanian-Najafabadi*[2], *Jila Ghazzavi*[1]

[1]*Department of Pharmaceutics, School of Pharmacy and Novel Drug Delivery Systems Research Centre, Isfahan University of Medical Sciences, Isfahan, Iran*
[2]*Department of Pharmaceutical Biotechnology, School of Pharmacy, Isfahan University of Medical Sciences, Isfahan, Iran*
✉ *E-mail: varshosaz@pharm.mui.ac.ir*

Abstract: The purpose of this study was to design a targeted anti-cancer drug delivery system for breast cancer. Therefore, doxorubicin (DOX) loaded poly(methyl vinyl ether maleic acid) nanoparticles (NPs) were prepared by ionic cross-linking method using Zn^{2+} ions. To optimise the effect of DOX/polymer ratio, Zn/polymer ratio, and stirrer rate a full factorial design was used and their effects on particle size, zeta potential, loading efficiency (LE, %), and release efficiency in 72 h (RE_{72}, %) were studied. Targeted NPs were prepared by chemical coating of tiptorelin/polyallylamin conjugate on the surface of NPs by using 1-ethyl-3-(3-dimethylaminopropyl) carboiimid HCl as cross-linking agent. Conjugation efficiency was measured by Bradford assay. Conjugated triptorelin and targeted NPs were studied by Fourier-transform infrared spectroscopy (FTIR). The cytotoxicity of DOX loaded in targeted NPs and non-targeted ones were studied on MCF-7 cells which overexpress luteinizing hormone-releasing hormone (LHRH) receptors and SKOV3 cells as negative LHRH receptors using Thiazolyl blue tetrazolium bromide assay. The best results obtained from NPs prepared by DOX/polymer ratio of 5%, Zn/polymer ratio of 50%, and stirrer rate of 960 rpm. FTIR spectrum confirmed successful conjugation of triptorelin to NPs. The conjugation efficiency was about 70%. The targeted NPs showed significantly less IC_{50} for MCF-7 cells compared to free DOX and non-targeted NPs.

1 Introduction

Breast cancer is currently one of the most frequently recognised cancers and the second most common cause of cancer death in women [1, 2]. Nowadays, chemotherapy including adjuvant and neo adjuvant chemotherapy is the major treatment for breast cancer and the standard treatment for this disease such as doxorubicin (DOX), paclitaxel, capecitabin, 5-fluoroucil, gefitinib, ixabepilone and everolimus [3–5].

DOX is one of the most active and widely used anti-cancer agents which inhibit the synthesis of nucleic acid within cancer cells [5]. It is used for treatment of solid cancer (such as breast and ovarian tumours) and leukaemia [6]. Despite the success of DOX against many cancers, effective doses of that shows significant side effects such as mylosuppression and cardiovascular toxicity, due to it's no specificity in inducing cell death [7, 8].

In recent years, cancer researchers have focused on more selective, targeted drug delivery based on Paul Ehrlich's idea of 'magic bullets' that would reduce toxic effects on normal cells and improve drug efficacy [9, 10].

Peptide receptors, which are expressed in large quantities on tumour cells are actually a mean of targeted drug delivery to malignant tumours. The luteinizing hormone-releasing hormone (LHRH) is a produced decapeptide hormone in the hypothalamus, which regulates the pituitary–gonadal axis, so it affects on the reproduction. Receptors of LHRH show increased expression in breast cancer cells, ovarian, endometrial and prostate, but on the contrary these receptors do not increase diagnosable in healthy organs cell [11, 12], so they can act as a targeting factor and absorption enhancer of anti-cancer drug in LHRH-positive cancer cells as well.

Many studies have been done on the field of using this peptide and its analogues as a targeting factor. Nagy and Schally [13, 14] used LHRH and its analogue as vector carrier to carry cytotoxic factors such as platinum and DOX which were chemically bound to peptide. All of these conjugates were bound to LHRH receptors *in vitro* and had greater anti-proliferative effects compared to the form of non-targeted drug [15, 16]. LHRH can be attached to colloidal systems such as dendrimers or nanoparticles (NPs) as a targeting agent [17, 18]. Minko *et al.* [19] developed a conjugated form of LHRH in polyamide and dendrimer amine with paclitaxel. It was shown that the conjugate was effectively internalised into cells and reduced the adverse effects of this drug [20]. Taheri *et al.* [21] also used this peptide for targeting methotrexate-human serum albumin NPs. LHRH targeted treatment was studied in a group of mice that were injected with 4T1 breast cancer cells. By 7 days after treatment, average tumour volume in the targeted NPs treated group decreased to 8.67% of the initial tumour volume while the average tumour volume in non-targeted NPs treated mice grew rapidly and reached 250.7% of the initial tumour volume [22]. LHRH–Fe_3O_4 NPs in the treatment of two separate breast tumour cell lines (MCF-7 and MDA-MB231) resulted in 95–98% cell death while no change in cell proliferation or cell apoptosis was observed in cells treated with equal amounts of either LHRH or un-conjugated Fe_3O_4 NPs [23, 24].

A great number of studies have been conducted on the targeting the DOX to a target organ to decrease its side effects and prevent of increasing its toxic dose.

Poly(methyl vinyl ether maleic acid) (PMVEMA) is a biocompatible copolymer widely used in the pharmaceutical applications. It is generally recognised as a safe excipient and is applied as denture adhesives, thickening and suspending agents and transdermal adjuvants. Recently, it was found that nanoparticulate systems based on PMVEMA were suitable for drug or antigen oral delivery due to the bioadhesive properties provided by PMVEMA which extended the gastrointestinal retention of drug loaded

nanoparticles effectively. Moreover, this capability of bioadhesion could be improved when particulate systems were coated with some excipients like bovine serum albumin, poly(ethylene glycol) or dextran. Finally, the acidic groups in PMVEMA have good capability for multi-functional modifications with hydroxyl (polyethylene glycol) or amino groups (polyethyleneimine) [25]. This polymer has been used in production of different nanoparticulte delivery systems in cell encapsulation [26] and controlled protein release [27]. PMVEMA-functionalised porous silicon nanoparticles have been used for enhanced stability and cellular internalisation [28].

The loading possibility of DOX in the form of hydrochloride salt in most of polymers which are soluble in organic solvents is low. Therefore, in this study, we tried to encapsulate this drug in the water soluble polymer of PMVEMA [29, 30] to eliminate the problem of the remaining of organic solvents used in emulsion solvent evaporation method and also enhance the loading efficacy of the drug in NPs. To control the drug release profile, cross-linking of the polymer with zinc sulphate was used. The purpose of this study was the use of PMVEMA NPs in preparing a targeted drug delivery system for efficient treatment of breast cancer. With respect to the high expression of LHRH receptors in breast cancer cells, which are absent in normal cells [11, 12], the target NPs were prepared by conjugation of triptorelin, a synthetic analogue of LHRH, to the NPs. To our knowledge, there is no report available about the coating of PMVEMA NPs with this peptide.

2 Materials and methods

2.1 Materials

DOX hydrochloride was provided by Hangzhou ICH Biopharm Co., Ltd (Zhejiang, China). PMVEMA (MW 80,000 Da), poly (allylamine hydrochloride) (MW 15,000 Da) and Coomassie Brilliant Blue G-250 dye were purchased from Aldrich (USA). 1-ethyl-3-(3-dimethylaminopropyl) carboiimid HCl (EDC), Zinc sulphate, NaOH, Thiazolyl blue tetrazolium bromide (MTT) and Tween 20 were from Merck Chemical Company (Germany). Orthophosphoric acid 85% w/v was from Panreac (Spain). MCF-7 and SKOV-3 cell lines were from the Pasteur Institute (Iran). Tripsin/EDTA and PRMI 1640, streptomycin/penicillin and FBS (foetal bovine serum) were purchased from Biosera Europe, ZI du Bousquet, France.

2.2 Preparation of DOX loaded PMVEMA NPs

NPs were prepared by an ionic cross-linking method of PMVEMA. For this purpose, 250 mg of PMVEMA was dissolved in 5 ml of deionised water on a magnetic stirrer (IKA-WERKE, Model RT 10 power, Japan) at room temperature. The speed of the stirrer was set at 450 rpm. 20 min later when it dissolved completely, the pH of the solution was adjusted to 7.4 by adding NaOH. Then DOX (6.25 or 12.5 mg) was added to this solution while it was stirred. Afterward, the solution of 125 mg of $ZnSO_4$ in 2.5 ml of deionised water was prepared and added drop wise with an insulin syringe to the polymer/drug solution in different stirring rates (according to Table 1). The curing time was 5 min. A two level factorial design was used for preparation of DOX loaded NPs. Three different variables including drug content (5 or 10% w/w of polymer), stirring rate (960 or 1200 rpm) and the amount of $ZnSO_4$ (25 or 50% w/w of the polymer) were studied (Table 1)

Table 1 Studied variables in factorial design used in preparation of DOX loaded PMVEMA NPs

Studied variables	Level 1	Level 2
drug/polymer ratio, w/w %	2.5	5
$ZnSO_4$/polymer ratio, w/w %	25	50
stirring rate, rpm	960	1200

Table 2 Composition of different formulation of DOX loaded PMVEMA NPs designed by full factorial design

Formulation code	DOX/polymer ratio (D), w/w %	ZnSO4/polymer ratio (Zn), w/w %	Stirring rate (R), rpm
$D_{2.5}Zn_{50}R_{960}$	2.5	50	960
$D_{2.5}Zn_{25}R_{960}$	2.5	25	960
$D_{2.5}Zn_{25}R_{1200}$	2.5	25	1200
$D_{2.5}Zn_{50}R_{1200}$	2.5	50	1200
$D_5Zn_{25}R_{1200}$	5	25	1200
$D_5Zn_{50}R_{1200}$	5	50	1200
$D_5Zn_{25}R_{960}$	5	25	960
$D_5Zn_{50}R_{960}$	5	50	960

and eight different formulations (Table 2) were designed by Design Expert Software (Version 7.1, USA).

2.3 Particle size and zeta potential measurements

The mean particle size (z-average) and zeta potential of DOX loaded NPs were measured by Zetasizer (Zetasizer 3600, Malvern Instrument Ltd, Worcestershire, UK) at 25°C. All particle size determinations were done in deionised water using a He-Ne laser beam at 658 nm with a scattering angle of 90°.

2.4 Determination of drug loading efficiency

Drug loading efficiency percent (LE %) was measured after centrifuging (Eppendorf AG 23331, model 5430, Hamburg, Germany) of NPs dispersion using Amicon Ultra-15 Centrifugal Filter Units (10 kDa MW cutoff, Millipore, Ireland). This process separated the plaque of nanoparticles from the aqueous solution which contained the un-entrapped free drug. Therefore, 1 ml of the drug loaded NPs was centrifuged at 11,180 g for 10 min. The separated aqueous solution was diluted with distilled water in the ratio of 1:10 and the concentration of free DOX was measured by a UV–vis spectrophotometer (UV-mini-1240 CE-Shimadzu, Japan) at $\lambda_{max} = 247$ nm [29]. Unloaded NPs were used as blank. Loading efficiency was calculated by using the following equation

$$\text{Drug loading efficiency (LE \%)} = \frac{\text{total drug} - \text{drug supernatant}}{\text{total drug}} \times 100 \quad (1)$$

2.5 In vitro release of DOX from NPs

The release of DOX from NPs was measured by the dialysis method, in phosphate buffer solution (PBS) 0.05 M (pH 7.4) containing 2% of Tween 20 (to mimic sink condition and prevent the saturation of the release medium). One millilitre of NPs dispersion of each formulation was transferred into dialysis membrane bags (MW cutoff 12 kDa, Memberacel®, Viskase, USA) and the bag was placed in 74 ml of release medium at 37°C while being stirred on magnetic stirrer. At determined time intervals, the concentration of DOX released in the medium was measured spectrophotometerically at $\lambda_{max} = 499.4$ nm. The same procedure was carried out for blank samples. To compare the release profiles, release efficiency within 72 h (RE_{72}%) parameter was used

$$RE_{72}\% = \frac{\int_0^t \cdot \mathrm{d}t}{y_{100} \cdot t} \times 100 \quad (2)$$

To find the kinetic model of drug release from NPs, mathematical analysis was done by the best curve fitting model; to zero-order, first-order, Baker–Lonsdale and Higuchi models

$$\text{Zero-order: } M_t = M_0 - K_0 t \quad (3)$$

$$\text{First-order: } \mathrm{Ln}\, M_t = \mathrm{Ln}\, M_0 - K_1 t \quad (4)$$

$$\text{Higuchi model: } M_t = K_h \times \sqrt{t} \quad (5)$$

$$\text{Baker-Lonsdale model: } \frac{3}{2}\left[1 - \left(1 - \frac{\mathrm{M_t}}{\mathrm{M_\infty}}\right)^{(2/3)}\right] - \frac{\mathrm{M_t}}{\mathrm{M_\infty}} = \mathrm{Kt} \quad (6)$$

In all these equations, M_t is the amount of drug released in time t, M_0 is the amount of initially applied drug, M_∞ is the drug release at infinite time and K is the drug release rate constant that is shown according to kinetic models as K_0, K_1, K_h and so on. Correlation coefficient for the linear regression may be used as a mean of comparing the 'quality of fit' to the different models.

2.6 Preparation of triptorelin/polyallylamine conjugate

For this purpose, triptorelin and EDC were dissolved in the same quantity in 1 ml of deionised water. Then, the solution was stirred for 3 h. Afterward 2 ml of an aqueous solution of polyallylamine with concentration of 1.25% was added to the solution of triptorelin (polyallylamine/triptorelin w/w% ratio 10:1). The resulted solution was stirred in darkness and water-ice bath for 15 h. Then, it was dialysed in 100 ml of deionised water to remove the EDC and unreacted triptorelin. The resulting connection was verified by Fourier-transform infrared spectroscopy (FTIR). A blank sample (a solution of polyallylamine with EDC) was prepared by the same process.

2.7 Preparation of Bradford reagent

The Bradford Comassie Brilliant Blue assay is a spectrophotometerical analysis method for determining the concentration of protein in solution. It is based on the binding of dye Coomassie Brilliant Blue G-250 dye to protein in acidic solution. For preparation of Bradford solution (5X), briefly, 125 mg of dark purple powder of Comasie Brilliant Blue G-250 was dissolved in 62.5 ml of 96% ethanol on stirrer, and 125 ml of orthophosphoric acid 85% w/v was added to this solution. The resulting solution was diluted with water to a final volume of 250 ml while the pH was less than 4 [31].

2.8 Determination of conjunction efficiency of triptorelin/polyallylamine

After dialysis of the synthesised sample, the un-reacted triptorelin was measured by the Bradford assay. For this purpose, 200 µl of the Bradford reagent was added to 800 µl of the dialysis medium solution. The absorption of the resulted solution was measured at $\lambda_{max} = 596.6$ nm. The mentioned steps were performed for the resulted solution of blank preparation too. The conjugation efficiency was calculated from (6) of the standard curve of measuring different concentrations of triptorelin against the absorbance after addition of the Bradford reagent

$$Y = 0.018x + 0.131 \quad (7)$$

where Y is the absorbance and x is the concentration (µg/ml).

2.9 Coating the conjugate of triptorelin/polyallylamine on the surface of NPs

The amine groups of the conjugated triptorelin/polyallylamine were attached to carboxylic acid groups of PMVEMA NPs by a chemical amidification reaction using EDC. For this purpose, the solution of conjugated triptorelin/polyallylamine was added drop wisely to the NPs dispersion (NPs polymer ratio to conjugated triptorelin/polyallylamine was 9:1 w/w %). EDC was added to the solution at the same quantity as triptorelin/polyallylamine. The resulted solution was vortexed about 2 h in darkness. Purification process was performed by using an Amicon Eppendorf tube (cutoff 100 kDa) to remove un-reacted conjugate of teriptorelin/polyallylamine and EDC. A blank solution was prepared by the same method. The samples were frozen at −20°C for 24 h and then were freeze-dried (Christ Alpha 2-4 LD Plus, Germany) at 0.001 mbar pressure for 48 h. The resulting products were analysed by FTIR.

2.10 Morphology of NPs

The morphology of the optimal formulation of DOX loaded NPs was evaluated by transmission electron microscope (TEM) (Zeiss, EM10C, Germany). For this work, at first a droplet of the NPs suspension was placed on a 300 mesh carbon copper grid and allowed to be dried normally at room temperature, then the micrographs with different levels of magnification were taken at an accelerating voltage of 80 kV.

2.11 Cell culture

MCF-7 and SKOV3 cell lines which are LHRH receptor positive and negative, respectively, were chosen for this study. The cells were cultured in PRMI 1640 containing 10% FBS and 1% antibiotics (mixture of penicillin 5000 U/ml and streptomycin 5000 µg/ml) at 37°C under 5% CO_2 atmosphere. For each cell line, first, 180 µl of the cell suspension at the density of 5×10^4 cells/ml were seeded into each well of 96-well culture plate (Singapore) and incubated for 24 h at 37°C in 5% CO_2 with an appropriate humidity before the cell viability test.

2.12 Cell viability assay

The cell viability was measured by MTT assay for both cell lines to compare the cytotoxic effect of free DOX with DOX loaded targeted and non-targeted NPs *in vitro*. After cells were seeded on 96-well plate, each row was treated with 20 µl of 0.2–1.6 µM concentration of free DOX (as a positive control), 20 µl of 0.1–1.6 µM non-targeted NPs with or without DOX, 20 µl of 0.05–1.6 µM concentration of targeted NPs with or without DOX and 20 µl of culture medium (as a negative control). Afterward, the plate was incubated for 48 h and then 20 µl MTT solution (5 mg/ml) was added to each well. Following 3 h of incubation, the cell medium was removed and 150 µl DMSO was added to each well to solubilise formazan crystals. Finally, the plate was subjected to absorbance read at 570 nm with a microplate reader. All experiments were performed in triplicate. Cell viability for each sample was calculated by using the following equation

$$\text{Cell survival\%} = \frac{(\text{mean of each group-mean of blank})}{(\text{mean of negative control-mean of blank})} \times 100 \quad (8)$$

2.13 Statistical analysis

Designing and optimisation of the NP formulations were done by Design Expert Software (version 7.1, Stat-Ease, Inc., Minneapolis, MN, USA) to get the main effects and the interaction effects of the studied factors on each response independently. SPSS software (version 20, IBM, USA) was used for statistical analysis of cell culture data. The cell culture data were shown as mean ± SD and compared by analysis of variance (ANOVA) test, followed by the LSD post hoc. $p < 0.05$ was considered significant in all cases.

3 Results and discussion

The physicochemical properties the studied formulations of NPs loaded with DOX are displayed in Table 3. The contribution effect of different independent parameters on the dependent parameters

Table 3 Physicochemical properties of DOX loaded PMVEMA NPs

Formulation code	Particle size, nm	Zeta potential, mV	Drug loading efficiency, %	Drug release efficiency (RE_{72}%)
$D_{2.5}Zn_{50}R_{960}$	247.50 ± 9.03	−23.1 ± 1.2	92.74 ± 5.26	27.73 ± 1.54
$D_{2.5}Zn_{25}R_{960}$	261.83 ± 30.60	−38.0 ± 2.3	90.70 ± 1.78	37.69 ± 2.23
$D_{2.5}Zn_{25}R_{1200}$	227.67 ± 11.62	−28.9 ± 1.5	92.59 ± 4.41	30.14 ± 2.41
$D_{2.5}Zn_{50}R_{1200}$	162.96 ± 1.60	−32.0 ± 0.4	90.79 ± 1.14	26.61 ± 3.27
$D_5Zn_{25}R_{1200}$	285.26 ± 26.25	−31.4 ± 1.7	91.39 ± 1.79	22.14 ± 2.12
$D_5Zn_{50}R_{1200}$	178.20 ± 24.15	−30.1 ± 3.7	91.48 ± 0.47	23.86 ± 2.31
$D_5Zn_{25}R_{960}$	223.80 ± 1.91	−32.8 ± 0.6	91.74 ± 0.71	20.77 ± 3.11
$D_5Zn_{50}R_{960}$	149.90 ± 5.31	−28.2 ± 2.0	90.77 ± 0.34	22.55 ± 2.95

or responses of particle size, zeta potential, drug loading efficiency and release efficiency are shown in Fig. 1.

3.1 Particle size

Table 3 shows the particle size changed between 149.90 ± 5.31 and 285.26 ± 26.25 nm in different formulations. The Zn/polymer ratio was the most important parameter affecting the size of NPs (Fig. 1). By increasing the Zn/polymer ratio the particle size became smaller (Fig. 2). However, it had no significant effect ($p > 0.05$) on the particle. Mathematical equation was generated by Design Expert® software for the model which assists in determining the effect of independent variables. In this equation, the positive sign indicates the parameter enhances the response, but the negative sign denotes a lowering effect on it. The final equation in terms of coded factors for particle size was obtained as

$$\text{Particle size} = 212.92 - 3.63A + 0.57B - 28.30C + 21.87AB - 16.95AC - 14.65BC$$

In which A is the drug/polymer ratio, B is the stirrer speed and C is the Zn/polymer ratio.

It shows that stirrer speed had synergistic (increasing) effect, but DOX/polymer and Zn/polymer ratio have an antagonist (decreasing) effect on the particle size of NPs. However, none of the factors studied had a significant effect on the particle size of the nanoparticles.

By increasing the Zn/polymer ratio, more electrostatic interactions may be formed between the polymer and cross-linking agent, the polymer chains will be interwoven and consequently the engaged and shrunk NPs result in smaller particle size. Yousefpour *et al.* [32] showed that by higher drug content and cross-linking agent the more compressed aggregation of conjugates created as more portion of the conjugated chain of polymer participated in inner hydrophobic interactions and as a result a smaller nanoaggregate size formed.

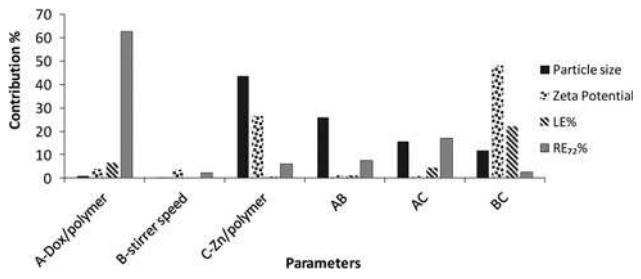

Fig. 1 *Contribution of different effective factors on the particle size, zeta potential, drug loading efficiency (LE%), drug release after 72 h (RE_{72}%)*

3.2 Zeta potential

Table 3 and Fig. 1 show the most effective parameter on the zeta potential was Zn/polymer ratio (while not significant). Although Fig. 1 shows neither A, B or C contribute significantly to the zeta potential, but it is shown that BC has a ∼50% contribution to the zeta potential. This means that when both these variables are changed meanwhile with each other their interaction effect will be very important to the zeta potential of the particles. This response varied between −23.1 ± 1.2 and −38.05 ± 2.3 mV. By increasing the Zn/polymer ratio the absolute value of zeta potential decreased (Fig. 2). The increasing of Zn/polymer ratio may cause more cross-linking reaction and electrical contacts between the COO^- group of PMVEMA and positively charged zinc ions, so negative charge of the COOH group of the polymer is neutralised and the absolute value of zeta potential is decreased. This result is consistent with other studies. For example, Arbos and Companero's study [33] showed that by increasing the 1, 3-diamino propene as cross-linker the zeta potential of PVM/MA NPs decreased.

3.3 Loading efficiency of DOX in NPs

As seen in Table 3 LE% changed between 90.70 ± 1.78 and 92.74 ± 5.26%. The mathematical equation proposed by the software for estimation of the LE% by changes of the coded independent parameters was

$$\text{Loading efficiency}\,\% = 91.55 - 0.20A + 0.016B - 0.054C + 0.081AB - 0.16AC - 0.37BC$$

This equation indicates that DOX/polymer and Zn/polymer ratio had antagonist or decreasing effect on the LE%, while stirrer speed had a synergistic or increasing effect on it. However, none of the variables studied had significant effects on a LE% ($p > 0.05$) (Fig. 1). High concentration of the polymer which prevents escaping of the entrapped drug from the nanoparticles and also the ionic interaction between the anions of the polymer and the cations of DOX which strongly bounds the drug to the polymeric nanoparticles might be the reasons of high loading efficiency of the drug in the NPs.

3.4 In Vitro release of DOX from NPs

Fig. 3 shows the release profiles of DOX against time for each nanoparticle formulation in phosphate buffer solution (pH 7.4) containing 2% Tween 20 in 37°C for 72 h. Drug release can take place by five different models: (i) excretion of the drug bound to the surface, (ii) diffusion through the nanoparticle matrix, (iii) diffusion through the polymer wall of nanocapsules, (iv) nanoparticle matrix erosion, or (v) a combined erosion–diffusion procedure [34, 35]. In all studied formulations, the release profile was prolonged (Fig. 3) so that in $D_{2.5}Z_{50}R_{960}$ NPs which showed the highest release rate, after 72 h only 47% of the drug was released. This may be related to the high concentration of the polymer and cross-linking agent, and also the ionic interaction between the anions of the polymer and the cations of DOX which caused strong bond between the polymer and the drug. The other parameter which influenced on the RE_{72}%, although to a lesser extent compared to the ratio of the drug/polymer, was the Zn/polymer ratio (Fig. 1). By increasing the Zn/polymer ratio the RE_{72}% decreased (Fig. 2). This phenomenon can be explained so that as mentioned earlier the particle size became bigger by decreasing the cross-linking agent concentration (Fig. 2) and therefore the aggregation of NPs probably ejected the trapped drug out of the polymer and drug release improved, therefore the RE_{72}% increased.

Table 4 shows by comparing the correlation coefficient data of drug release profiles from all studied formulations fitted with different release kinetic models better fit with the Baker–Lonsdale model.

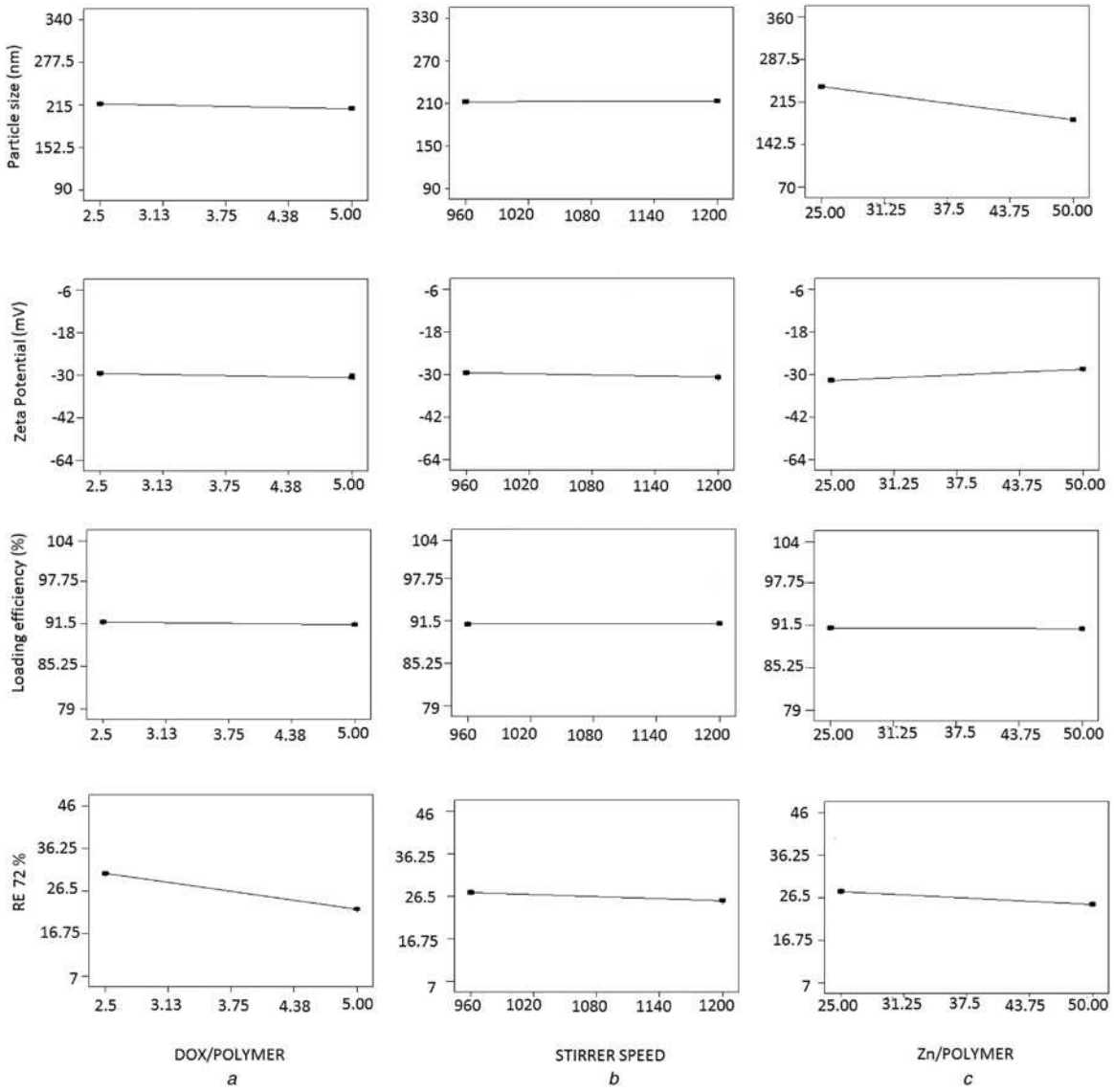

Fig. 2 *Effect of different levels of studied parameters on the particle size, zeta potential, loading efficiency and drug release efficiency of DOX loaded PMVEMA NPs*

3.5 Optimisation of the formulation of NPs

The computer optimisation process by Design Expert Software was carried out and a desirability function determined the effect of the levels of independent variables on the studied responses. The constraints of particle size, zeta potential, loading efficiency and RE_{72}% were $149.9 \leq Y1 \leq 285.26$ nm, $-23.1 \leq Y2 \leq -38.05$ mV, $90.7 \leq Y3 \leq 92.74\%$ and $20.77 \leq Y4 \leq 37.69\%$, respectively. The targets of all studied variables were set at the range of the obtained data. Considering the data of Table 3 optimisation was carried out by Design Expert Software and the optimised nanoparticle formulation suggested by desirability of 100% was $D_5Zn_{50}R_{960}$ formulation which was prepared by stirring rate of 960 rpm, Zn/polymer ratio of 50% and DOX/polymer ratio of 5%.

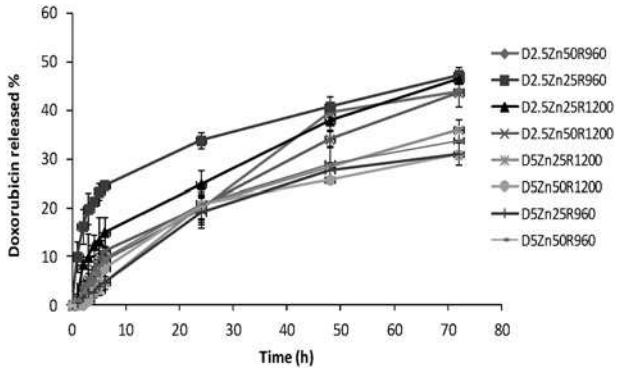

Fig. 3 *DOX release profile from different studied PMVEMA NPs*

3.6 Conjugation of triptorelin/polyallylamine

To attach the LHRH agonist (triptorelin) to polyallylamine, EDC was used as a cross-linker, which could create amide linkage between the

Table 4 Correlation coefficient of different kinetic models obtained by curve fitting method to DOX HCl release data from NPs

Formulation	Zero order	First order	Higuchi model	Baker-Lonsdale model
$D_{2.5}Zn_{50}R_{960}$	0.9640	0.8639	0.9600	0.9710
$D_{2.5}Zn_{25}R_{960}$	0.6501	0.6961	0.7892	0.8320
$D_{2.5}Zn_{25}R_{1200}$	0.9262	0.8676	0.9733	0.9941
$D_{2.5}Zn_{50}R_{1200}$	0.9508	0.8503	0.9789	0.9818
$D_5Zn_{25}R_{1200}$	0.9609	0.8325	0.9612	0.9937
$D_5Zn_{50}R_{1200}$	0.9130	0.6705	0.9445	0.9888
$D_5Zn_{25}R_{960}$	0.9386	0.8193	0.9511	0.9902
$D_5Zn_{50}R_{960}$	0.9215	0.7856	0.9612	0.9902

IET Nanobiotechnol., 2016, Vol. 10, Iss. 4, pp. 206–214

amino groups of polyallylamine and COOH groups of triptorelin. The conjugation was confirmed by analysis of FTIR. Figs. 4*a–c* show FTIR spectra of triptorelin, polyallylamine and their conjugation, respectively. In the spectrum of triptorelin, the OH bond of carboxylic acid is seen around 3302.5 cm^{-1} (3400–2400 cm^{-1}) (Fig. 4*a*) and the N–H stretching bond of the primary amines of polyallylamine spectrum seen in 3468.35 cm^{-1} (Fig. 4*b*) are replaced with the N–H bond of the produced amide seen in 3439.42 cm^{-1} in the conjugate spectrum (Fig. 4*c*). Also the peaks related to the N–H bending bonds of polyallylamine which are not involved in the reaction are seen in 1608.34 cm^{-1} in the spectrum of the conjugate (Fig. 4*c*). In triptorelin, spectrum stretching C=O bond of amide groups of the peptide are seen in 1660.41 cm^{-1} (1680–1630 cm^{-1}) (Fig. 4*a*) and in polyallylamine spectrum N–H bending bond is seen in 1611.23 cm^{-1} (1640–1500 cm^{-}) (Fig. 4*b*).

3.7 Conjugation efficiency of triptorelin/polyallylamine measurement

Respected to the molecular weight of triptorelin and polyallylamine (~1300 against 17,500 Da), after dialysis of the synthesised sample of triptorelin/polyallylamine (cutoff 12,000 Da) the un-reacted triptorelin which comes out of the dialysis membrane was measured by the Bradford assay spectrophotometrically in λ_{max} = 596.6 nm using equation ($y = 0.018x + 0.131$) obtained from the

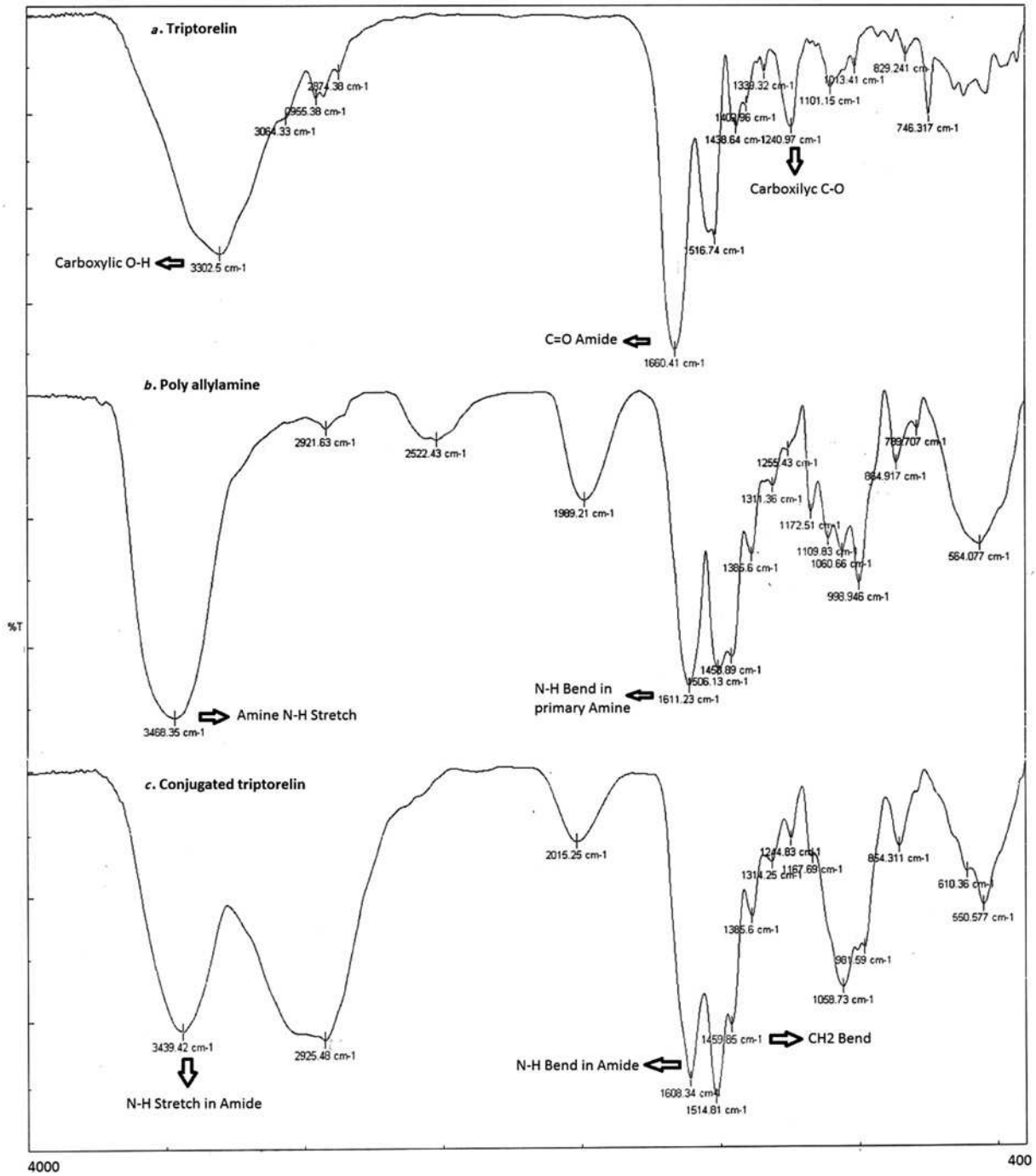

Fig. 4 *FTIR spectrum of*

a Triptorelin
b Polyallylamine
c Conjugated triptorelin/polyallylamine

calibration curve of triptorelin. The results showed about 70% of triptorelin was conjugated to polyallylamine.

3.8 Coating of the NPs by conjugated triptorelin/polyallylamine

Coating of the conjugated triptorelin/polyallylamine on the surface of NPs was conducted by the chemical reaction using EDC to cross-link the bonds between amine groups of the conjugated triptorelin/polyallylamine and free COOH groups of NPs. FTIR analysis of NPs and the coated NPs are shown in Fig. 5. As it can be seen in the spectra of the coated NPs an additional peak in 1623.77 cm^{-1} was added compared to non-coated NPs spectra that may be referred to the C=O bond of the formed amide group. Also the peak in 1592.91 cm^{-1} in non-coated NPs spectra was replaced with a peak in 1566.9 cm^{-1} in coated NPs which is related to the N–H bond of the amide group. A C–N stretching bond of amines related to polyallylamine attached to triptorelin is seen in 1090.55 cm^{-1} in coated NPs.

3.9 Transmission electron microscopy

Fig. 6 shows the TEM micrographs of the optimum formulation of DOX loaded NPs. This figure shows the sphericity of the NPs although the particle size is not in good accordance with the results of dynamic light scattering (DLS) tests. Hydrodynamic diameter and size polydispersity can be obtained directly in water or in an isotonic buffer by DLS. The parameter measured by DLS is the equivalent sphere translational diffusion coefficient (*Do*). This coefficient is then placed directly into the Stokes–Einstein equation to obtain a hydrodynamic radius (R_h), where k is the Boltzmann constant, T is the absolute temperature and h is the viscosity of the solvent. An indication of NPs size may also be obtained through microscopy techniques with the understanding that the resulting sizes obtained may not be the actual hydrated diameters of NPs in solution, depending on the sample preparation methods required.

3.10 In vitro cytotoxicity

Adverse side effects of anticancer drugs on the healthy organs have limited their usage, so targeted drug delivery systems could decrease these problems. This strategy is based on the capability of targeting agents or ligands to bind to the tumour cell surface. The LHRH is one of the targeting agents that its receptor is over expressed on some tumour cells such as breast, ovarian, endometrial and prostate cancers [11, 12]. In this study, we focused on increasing cytotoxicity of DOX loaded PMVEMA NPs by employing triptorelin (synthetic LHRH analogue) as a tumour specific targeting moiety. So we hypothesised that targeted NPs could kill MCF-7 cells (which over expresses LHRH receptor) more specifically comparing to free DOX and non-targeted NPs. The results of our study confirmed this hypothesis. Fig. 7 shows the results of cell survival percentages of MCF-7 and LHRH receptor negative SKOV3 cells by the MTT assay. For being comparable, the DOX concentration in NPs was adjusted to be the same as the free DOX.

According to Fig. 7*a*, DOX loaded-targeted NPs showed significantly ($p < 0.05$) higher cytotoxicity than non-targeted NPs and free DOX on MCF-7 cells. In all concentrations, the cells treated with the targeted and non-targeted NPs showed significantly ($p < 0.05$) lower viabilities comparing to free DOX. However, in case of similar treatments of the LHRH-receptor negative SKOV3 cells, no significant difference was observed between the targeted and non-targeted NPs ($p > 0.05$). This experiment confirmed effective interaction between the LHRH on the surface of NPs and its receptors, which consequently results in increased cellular uptake via endocytosis. This facilitated the entrance of DOX in to the MCF-7 cells while in SKOV3 cells the cytotoxicity of DOX may be just related to the drug diffusion into the cells.

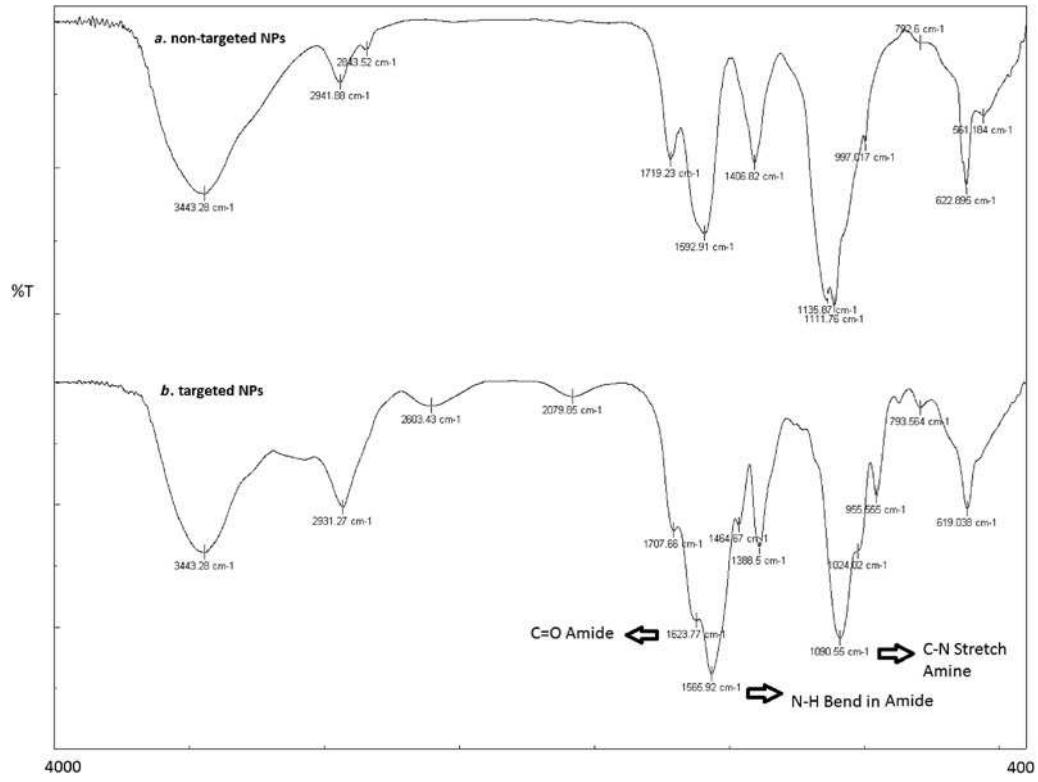

Fig. 5 *FTIR spectrum of*

a Non-targeted
b Targeted NPs

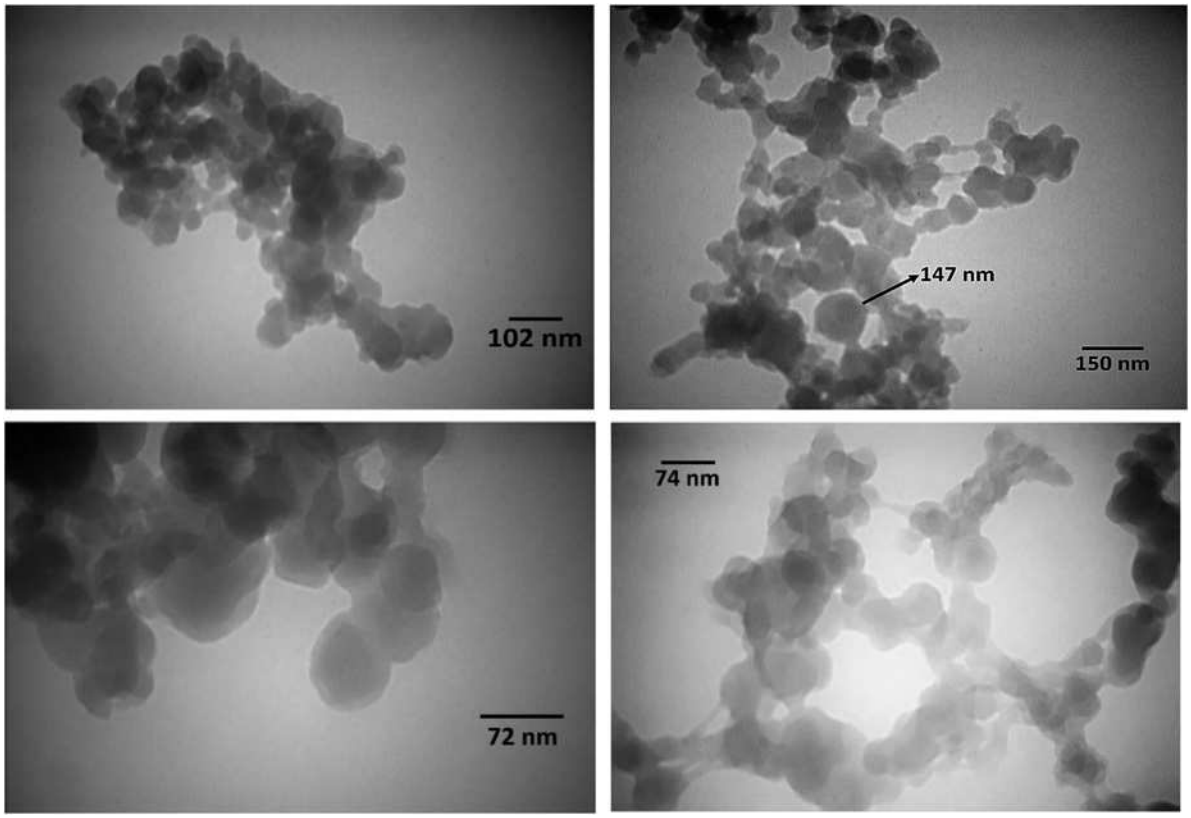

Fig. 6 *TEM micrographs of optimized formulation of doxorubicin loaded NPs*

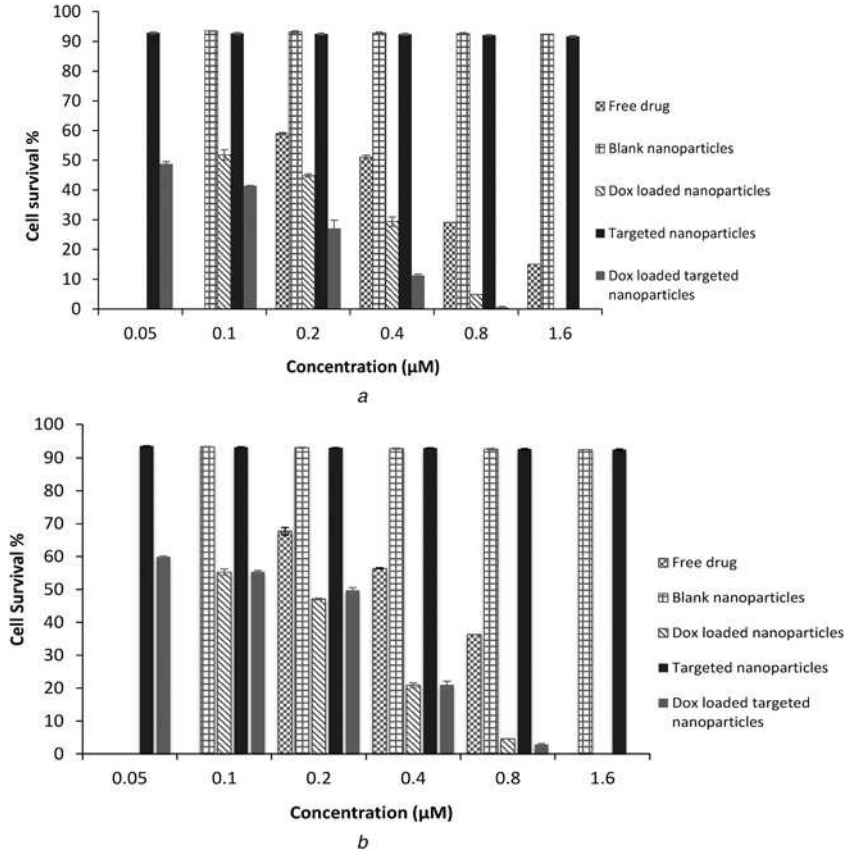

Fig. 7 *Viability of*

a MCF-7

b SKOV3 cells after treatment with different concentrations of targeted and non-targeted NPs with or without DOX compared to free DOX by MTT assay

Table 5 IC_{50} values of free DOX, or DOX loaded in non-targeted and targeted NPs on the MCF-7 (LHRH receptor-bearing) and SKOV3 cells (lacking LHRH receptor) after 72 h

Formulation	IC_{50}, μM	
	MCF-7	SKOV3
free drug	0.386 ± 0.025	0.542 ± 0.041
DOX loaded in non-targeted NPs	0.117 ± 0.022	0.128 ± 0.01
DOX loaded in targeted NPs	0.018 ± 0.008	0.155 ± 0.001

The IC_{50} of DOX as free drug, or drug loaded in targeted and non-targeted NPs are compared in Table 5. As this table indicates, the IC_{50} of DOX for MCF-7 cells in the case of targeted and non-targeted NPs were reduced 21 and 3 folds, respectively, comparing to the free DOX.

Taheri *et al.* [21] conjugated LHRH to methotrexate-human serum albumin (MTX-HAS) NPs via EDC as the cross-linker. They also showed significant cytotoxicity of the LHRH targeted NPs on the LHRH positive T47D cells compared to non-targeted NPs.

In another study, a synthetic analogue of LHRH peptide was attached to the nanocarriers containing paclitaxel. Intratumoral accumulation and anti-cancer efficacy of targeted nanocarriers were enhanced compered to non-targeted ones in the tumour of mice bearing xenografts of human A549 lung carcinoma [36].

4 Conclusion

In this study, DOX loaded NPs of PMVEMA were prepared by the cross-linking method. The effect of stirring rate, DOX/polymer and ZN/polymer ratio were studied in eight different formulations. Finally, the formulation prepared using 5% of DOX, 50% of $ZnSO_4$ and stirrer speed of 960 rpm was selected as the optimal formulation. Triptorelin/polyallylamine conjugation was prepared and coated on the surface of the NPs in order to carry out an active targeting procedure for drug delivery to cancerous breast cells. Targeted NPs containing DOX showed the highest significant cytotoxic effects on LHRH-positive MCF7 compared to the non-targeted NPs and free DOX. Also targeted and non-targeted DOX loaded NPs had almost the same cytotoxicity effect on SKOV3 cells (as negative non-bearing LHRH receptor cells). This confirmed the cellular uptake of the targeted NPs in MCF-7 cells via the receptor mediated endocytosis. It is notable that the blank NPs were not cytotoxic, which indicates the safety of the selected polymers. However, these observations must be further investigated in preclinical *in vivo* studies to confirm the specific cytotoxic effects of the targeted nanoparticles.

5 References

1 American Cancer Society: 'Breast cancer facts and figures 2011–2012' (American Cancer Society, Atlanta, Ga, USA, 2012)
2 Greenlee, R.T., Murray, T., Bolden, S., *et al.*: 'Cancer statistics', *CA Cancer J. Clin.*, 2000, **50**, pp. 7–33
3 Wang, X., Teng, Z., Wang, H.: 'Increasing the cytotoxicity of DOX in breast cancer MCF-7 cells with multidrug resistance using a mesoporous silica nanoparticle drug delivery system', *Int. J. Clin. Exp. Pathol.*, 2014, **7**, (4), pp. 1337–1347
4 Jones, K.L.: 'Breast cancer', in Alldrege, B.K., Corelli, R.L., Ernst, M.E. (Eds.): 'Koda-Kimble and Young's Applied Thrapeutics, the clinical use of Drugs' (Lippincott Williams and Wilkins, New York, 2012, 10th edn.), pp. 2129–2199
5 Brannon-Peppas, L., Blanchette, O.J.: 'Nanoparticle and targeted system for cancer therapy', *Adv. Drug Deliv. Rev.*, 2012, **64**, pp. 206–212
6 Cai, S., Thati, S., Bagby, T.R., *et al.*: 'Localized DOX chemotherapy with a biopolymeric nano carrier improves survival and reduce toxicity in xenografts of human breast cancer', *J. Control Release*, 2010, **146**, (2), pp. 212–218
7 Ganz, W.I., Sridhar, K.S., Ganz, S.S., *et al.*: 'Review of tests for monitoring DOX-induced cardiomyopathy', *Oncology*, 1996, **53**, (6), pp. 461–470
8 Wang, J.J., Cortes, E., Sinks, L.F., *et al.*: 'Therapeutic effect and toxicity of adriamycin in patients with neoplastic disease', *Cancer*, 1971, **28**, (4), pp. 837–843
9 Schally, A.V., Nagy, A.: 'Chemotherapy targeted to cancers through tumoral hormone receptors', *Trends Endocrinol. Metab.*, 2004, **15**, pp. 300–310
10 Schally, A.V., Nagy, A.: 'Cancer chemotherapy based on targeting of cytotoxic peptide conjugates to their receptors on tumors', *Eur. J. Endocrinol.*, 1999, **141**, pp. 1–14
11 Reubi, J.C.: 'Peptide receptors as molecular targets for cancer diagnosis and therapy', *Endocrinol. Rev.*, 2003, **24**, pp. 389–427
12 Leuschner, C., Hansel, W.: 'Targeting breast and prostate cancers through their hormone receptors', *Biol. Reprod.*, 2005, **73**, pp. 255–260
13 Nagy, A., Schally, A.: 'Targeted cytotoxic somatostatin analogs: a modern approach to the therapy of various cancers', *Drugs Future*, 2001, **26**, pp. 261–270
14 Nagy, A., Schally, A.: 'Cytotoxic analogs of luteinizing hormone-releasing hormone (LHRH): a new approach to targeted chemotherapy', *Drugs Future*, 2002, **27**, pp. 359–370
15 Ben-Yehudah, A., Lorberboum-Galski, H.: 'Targeted cancer therapy with gonadotropin-releasing hormone chimeric proteins', *Anticancer Ther.*, 2004, **4**, pp. 151–161
16 Leuschner, C., Enright, F., Gawronska-Kozak, B., *et al.*: 'Human prostate cancer cells and xenografts are targeted and destroyed through luteinizing hormone-releasing hormone receptors', *Prostate*, 2003, **56**, pp. 239–249
17 Qi, L., Nett, T., Allen, M., *et al.*: 'Binding and cytotoxicity of conjugated and recombinant fusion proteins targeted to the gonadotropin-releasing hormone receptor', *Cancer Res.*, 2004, **64**, pp. 2090–2095
18 Taratula, O., Garbuzenko, O.B., Kirkpatrick, P., *et al.*: 'Surface-engineered targeted PPI dendrimer for efficient intracellular and intra tumoral siRNA delivery', *J. Control. Rel.*, 2009, **140**, pp. 284–293
19 Minko, T., Patil, M.L., Zhang, M., *et al.*: 'LHRH-Targeted NPs for cancer therapeutics', *Methods Mol. Biol.*, 2010, **624**, pp. 281–294
20 Janaky, T., Juhasz, A., Bajusz, S., *et al.*: 'Analogues of luteinizing hormone-releasing hormone containing cytotoxic groups', *Proc. Natl. Acad. Sci. USA.*, 1992, **89**, pp. 972–976
21 Taheri, A., Dinarvand, R., Atyabi, F., *et al.*: 'Enhanced anti-tumoral activity of methotrexate-human serum albumin conjugated nanoparticles by targeting with luteinizing hormone-releasing hormone (LHRH) peptide', *Int. J. Mol. Sci.*, 2011, **12**, (7), pp. 4591–4608
22 Taheri, A., Dinarvand, R., Ahadi, F., *et al.*: 'The in vivo antitumor activity of LHRH targeted methotrexate–human serum albumin NPs in 4T1 tumor-bearing Balb/c mice', *Int. J. Pharm.*, 2012, **431**, (1–2), pp. 183–189
23 Leuschner, C., Kumar, C.S.S.R., Hansel, W., *et al.*: 'LHRH-conjugated magnetic iron oxide nanoparticles for detection of breast cancer metastases', *Breast Cancer Res. Treat.*, 2006, **99**, (2), pp. 163–176
24 Kakar, S.S., Jin, H., Hong, B., *et al.*: 'LHRH receptor targeted therapy for breast cancer', *Adv. Exp. Med. Biol.*, 2008, **614**, pp. 285–296
25 Zhang, D., Pan, X., Wang, S., *et al.*: 'Multifunctional poly(methyl vinyl ether-co-maleic anhydride)-graft-hydroxypropyl-beta-cyclodextrin amphiphilic copolymer as an oral high-performance delivery carrier of tacrolimus', *Mol. Pharm.*, 2015, **12**, pp. 2337–2351
26 Gardner, C.M., Burke, N.A., Chu, T., *et al.*: 'Poly(methyl vinyl ether-alt-maleic acid) polymers for cell encapsulation', *J. Biomater. Sci. Polym. Ed.*, 2011, **22**, pp. 2127–2145
27 Moreno, E., Schwartz, J., Larraneta, E., *et al.*: 'Thermosensitive hydrogels of poly (methyl vinyl ether-co-maleic anhydride) – Pluronic F127 copolymers for controlled protein release', *Int. J. Pharm.*, 2014, **459**, pp. 1–9
28 Shahbazi, M.A., Almeida, P.V., Makila, E., *et al.*: 'Poly(methyl vinyl ether-alt-maleic acid)-functionalized porous silicon nanoparticles for enhanced stability and cellular internalization', *Macromol. Rapid Commun.*, 2014, **35**, pp. 624–629
29 Varshosaz, J., Hasanzadeh, F., Sadeghi-Aliabadi, H., *et al.*: 'Synthesis of pluronic® F127-poly(methyl vinyl ether-alt-maleic acid) copolymer and production of its micelles for DOX delivery in breast cancer', *Chem. Eng. J.*, 2014, **240**, pp. 133–146
30 Varshosaz, J., Minayian, M., Forghanian, M.: 'Prolonged hypocalcemic effect by pulmonary delivery of calcitonin loaded poly (methyl vinyl ether maleic acid) bioadhesive nanoparticles', *Biomed. Res. Int.*, 2014, **2014**, Article. 932615, pp. 1–13
31 Varshosaz, J., Hassanzadeh, F., Sadeghi-Aliabadi, H., *et al.*: 'Synthesis of pluronic® F-127-poly(methyl vinyl ether-alt-maleic acid) copolymer and production of its micelle for DOX delivery in breast cancer', *Chem. Eng. J.*, 2014, **240**, pp. 133–146
32 Yousefpour, P., Atyabi, F., Farahani, E., *et al.*: 'Targeted delivery of DOX-utilizing chitosan NPs surface-functionalized with anti-Her2 trastuzumab', *Int. J. Nanomed.*, 2011, **6**, pp. 1977–1990
33 Arbos, P., Companero, M.A., Arangoa, M.A., *et al.*: 'Influence of surface characteristics of PVM/MA NPs on their bioadhesive properties', *J. Control. Rel.*, 2003, **89**, pp. 19–30
34 Kumari, A., Yadav, S.K., Yadav, S.C.: 'Biodegradable polymeric NPs based drug delivery systems', *Colloid. Surf. B, Biointerf.*, 2010, **75**, (1), pp. 1–18
35 Ringe, K., Walz, C., Sabel, B.: 'Nanoparticle drug delivery to the brain', in Nalwa, H.S. (Ed.): 'Encyclopedia of nanoscience and nanotechnology' (American Scientific Publishers, New York, 2004), vol. 7
36 Saad, M., Garbuzenko, O.B., Ber, E., *et al.*: 'Receptor targeted polymers, dendrimers, liposomes: Which nanocarrier is the most efficient for tumor-specific treatment and imaging?', *J. Control. Rel.*, 2008, **130**, (2), pp. 107–114